Author Manuscript

Author Manuscript

Author Manuscript

Author Manuscript

HHS Public Access

Author manuscript

J Neurophysiol. Author manuscript; available in PMC 2023 December 09.

Published in final edited form as:

J Neurophysiol. 2000 May ; 83(5): 2661–2675. doi:10.1152/jn.2000.83.5.2661.

Differences in Control of Limb Dynamics During Dominant and Nondominant Arm Reaching

R. L. SAINBURG,

D. KALAKANIS

School of Health Related Professions, State University of New York at Buffalo, Buffalo, New York 14214

Abstract

This study compares the coordination patterns employed for the left and right arms during rapid targeted reaching movements. Six right-handed subjects reached to each of three targets, designed to elicit progressively greater amplitude interaction torques at the elbow joint. All targets required the same elbow excursion (20°), but different shoulder excursions (5, 10, and 15°, respectively). Movements were restricted to the shoulder and elbow and supported on a horizontal plane by a frictionless air-jet system. Subjects received visual feedback only of the final hand position with respect to the start and target locations. For motivation, points were awarded based on final position accuracy for movements completed within an interval of 400–600 ms. For all subjects, the right and left hands showed a similar time course of improvement in final position accuracy over repeated trials. After task adaptation, final position accuracy was similar for both hands; however, the hand trajectories and joint coordination patterns during the movements were systematically different. Right hand paths showed medial to lateral curvatures that were consistent in magnitude for all target directions, whereas the left hand paths had lateral to medial curvatures that increased in magnitude across the three target directions. Inverse dynamic analysis revealed substantial differences in the coordination of muscle and intersegmental torques for the left and right arms. Although left elbow muscle torque contributed largely to elbow acceleration, right arm coordination was characterized by a proximal control strategy, in which movement of both joints was primarily driven by the effects of shoulder muscles. In addition, right hand path direction changes were independent of elbow interaction torque impulse, indicating skillful coordination of muscle actions with intersegmental dynamics. In contrast, left hand path direction changes varied directly with elbow interaction torque impulse. These findings strongly suggest that distinct neural control mechanisms are employed for dominant and non dominant arm movements. However, whether interlimb differences in neural strategies are a consequence of asymmetric use of the two arms, or vice versa, is not yet understood. The implications for neural organization of voluntary movement control are discussed.

Address for reprint requests: R. L. Sainburg, 90 Farber Hall, Main St. Campus, State University of New York at Buffalo, Buffalo, NY 14214.

The costs of publication of this article were defrayed in part by the payment of page charges. The article must therefore be hereby marked "*advertisement*" in accordance with 18 U.S.C. Section 1734 solely to indicate this fact.

Author Manuscript Author Manuscript Author Manuscript Author Manuscript

INTRODUCTION

Handedness, the manual asymmetry characterized by the tendency to favor one hand for performance of skilled unimanual tasks, is an intriguing feature of human motor performance. To investigate whether handedness is associated with asymmetries in neural control, previous studies compared dominant and nondominant arm performance during aimed movements. A number of studies showed that dominant arm advantages in reaching accuracy were not evident during "ballistic" (low precision, high speed) movements and only emerged when the precision requirements of the experimental task increased (Carson et al. 1993; Elliott et al. 1994; Flowers 1975; Steingruber 1975; Todor and Cisneros 1985). Some studies attributed better accuracy of the dominant arm, during higher precision movements, to less trajectory "corrections" during the deceleration phase (Carson et al. 1993; Todor and Cisneros 1985), whereas others attributed this accuracy advantage to smaller errors in the initial acceleration phase of motion (Annett et al. 1979; Roy and Elliott 1986). The former reports proposed a dominant arm advantage for error correction mechanisms, whereas the latter proposed that movement planning is more effective and consistent for the dominant arm. Studies that manipulated target information before movement onset reported longer reaction times for the dominant arm, further suggesting interlimb disparities in movement preparation (Carson 1992; Carson et al. 1990, 1995; Elliott et al. 1993).

Recent studies investigating control of multijoint coordination have indicated the importance of movement dynamics in understanding neural control of reaching movements. To produce a desired trajectory, muscle forces must be coordinated with both external forces, imposed by the environment, and additional internal forces that arise from within the musculoskeletal system. Internal forces include interaction forces imposed on a given limb segment by motion of the attached segments, and forces resulting from stretch and compression of noncontractile tissues. Environmental forces include those arising from sources external to the musculoskeletal system (i.e., gravity and contact with objects). Previous reports have shown that, with practice, using the dominant arm, subjects adapt to coriolis forces (Lackner and Dizio 1994) and viscous forces applied to the hand by a manipulandum (Gandolfo et al. 1996; Goodbody and Wolpert 1998; Shadmehr and Mussa-Ivaldi 1994). The use of anticipatory mechanisms for this adaptation was evident from the existence of "after effects," or hand path curvatures that mirrored the direction and magnitude of previously applied forces. We recently extended these findings by showing that control of interaction forces also relies on neural representations of musculoskeletal dynamics (Sainburg et al. 1999). After adaptation to a mass attached by an outrigger to the forearm, the position of the mass was experimentally manipulated (thus changing the center of mass of the forearm/mass segment) on random, "surprise" trials. During these trials, the subjects continued to initiate movements with muscle torque patterns appropriate to the previously adapted inertial condition. Errors in initial movement direction were thus accurately predicted by an open-loop forward simulation. These studies provided evidence that successful coordination of multisegment movements is dependent on accurate neural representations of musculoskeletal and task-specific dynamics.

Author Manuscript Author Manuscript Author Manuscript Author Manuscript

The purpose of this paper is to investigate dominant and nondominant arm differences in interjoint coordination during targeted reaching movements. We compare the performance of the dominant and nondominant arm during rapid aimed reaching movements of six neurologically intact, right-handed subjects. Both arms were supported in the horizontal plane by an air-jet system, which eliminated the effects of gravity and friction. Because motion of the arm was influenced by both muscle forces and intersegmental forces, we separately analyzed these effects as muscle torque and interaction torque (see Sainburg et al. 1999). To experimentally manipulate the intersegmental dynamic contributions to limb movement, we presented three targets of varying directions and distances, designed to require the same amount of elbow motion (20°) but varying amounts of shoulder motion (5, 10, and 15°). Thus we were able to investigate the effects of interaction torques on the control of voluntary reaching with the dominant and nondominant arms.

METHODS

Subjects and apparatus

Subjects were six, neurologically intact, right-handed adults (2 females, 4 males), 24–36 yr of age. All subjects scored 100 (laterality quotient) on the 10-item version of the Edinburgh inventory (Oldfield 1971). All subjects provided informed consent before participation in this study, which was approved by the institutional review board of the State University of New York at Buffalo. Figure 1 illustrates the experimental setup. Subjects sat facing a computer screen with each arm supported, over a horizontal table top at shoulder height, by a frictionless air-jet system. All joints distal to the elbow were immobilized using an air splint. The scapulae and trunk were immobilized using a custom-fit butterfly-shaped chest restraint. Precision, single turn, linear potentiometers (Beckman Instruments) were used to monitor the elbow and shoulder joint angles, and data were digitized using a Macintosh computer equipped with an A/D board (National Instruments PCI-MIO-16XE-50). The experimental tasks and hand position feedback were presented to the subjects using a second computer. The position of the index finger was calculated from joint angle data and limb segment lengths and was displayed as a screen cursor. Vision of the arm and tabletop was blocked using a horizontal screen. Computer algorithms for experiment control and data analysis were custom written.

Task

A starting circle (10 mm diam) was displayed on the lower part of the computer screen while one of three target circles (5 mm diam) was displayed on the top part of the screen (see Fig. 1). To control the rotational effects of upper arm motion on the forearm (interaction torque), we presented three targets that required the same elbow excursion (20°), but different shoulder excursions (*target 1* = 5°, *target 2* = 10°, *target 3* = 15°). Between trials, the hand position was shown in real time as a screen cursor. Before each trial, subjects were to hold the cursor within the starting circle for 1 s. The trial was then initiated by an audiovisual signal at which time the cursor was blanked. Subjects were instructed to move their hand to the target using a single, uncorrected, rapid motion.

Author Manuscript Author Manuscript Author Manuscript Author Manuscript

At the end of each trial, knowledge of results was provided in the form of a crosshair indicating final position. To motivate subjects, audiovisual feedback and points were awarded for accuracy when the movement occurred in a prescribed time window (400–600 ms). Movement initiation and termination were determined by analyzing the hand's tangential velocity profile. To account for small oscillations of the hand inside the starting circle, movement onset was defined to occur 10 ms before the last minimum (below 5% V_{max}) prior to the maximum (V_{max}) in the hand's tangential velocity profile. Final position was defined to occur 10 ms after the first minimum (below 5% V_{max}) following the peak in tangential hand velocity (see Fig. 2), thus requiring subjects to perform rapid, uncorrected movements. Subjects moved one hand at a time, alternating hands every 12 trials. Each experimental session consisted of 240 trials, in which the targets were presented in a continuous sequence (*target 1, target 2, target 3, target 1*. . .). The order of target presentation was randomized between subjects. Because not all trials were successfully completed, our analysis includes 230 trials from each subject. For motivation, points were awarded based on accuracy.

Kinematic analysis

The shoulder and elbow potentiometer signals were collected at 500 Hz, converted to joint angles, low-pass filtered at 20 Hz (3rd order, no-lag Butterworth), and double differentiated to yield angular velocity and acceleration values. Elbow (ϕ) and shoulder (θ) joint angles are defined in Fig. 1.

Hand paths were calculated from joint angle data using the measured length of the upper arm and the distance from the elbow to the index finger (proximal metacarpophalangeal joint). The angular data were transformed to a Cartesian coordinate system with the origin at the shoulder (see Fig. 1). For direct comparison between left and right hand trajectories, the left hand paths were converted to a "right-hand" coordinate system. Thus the medial to lateral axis is represented graphically from left to right for both hands (see Figs. 3 and 5A). Task accuracy was measured as the distance between the final position and the center of the target circle. Hand path "direction-change" was defined as the difference in direction (η) between the average velocity vectors calculated for the following two movement periods: *1*) movement initiation to time-of-peak tangential hand velocity (V_{max}) and *2*) time-of-peak tangential hand velocity (V_{max}) to movement termination. This measure provided a signed value indicating the overall direction-change between the acceleration and deceleration phases of motion (see Fig. 2).

Kinetic analysis

To separately analyze the effects of intersegmental forces and muscle forces on limb motion, we partitioned the terms of the equations of motion into three main components: interaction torque, muscle torque, and net torque. Interaction torque represents the rotational effect of the forces due to the motion of the segments about the joints. The muscle torque primarily represents the rotational effect of muscle forces. Finally, the net torque is directly proportional to joint acceleration, inversely proportional to limb inertia, and equal to the combined muscle and interaction torques (see Sainburg et al. 1999; Zajac and Gordon 1989).

Author Manuscript Author Manuscript Author Manuscript Author Manuscript

It is important to note that the computed muscle joint torque cannot be considered a simple proxy for the neural activation of the muscles acting at that joint. Muscle joint torque does not distinguish muscle forces that counter one another during co-contraction, and it also includes the passive effects of soft tissue deformation. Additionally, the force generated by muscle to a given neural input signal is dependent on muscle length, rate of muscle length change, and recent activation history, whereas the contribution of muscle force to joint torque changes with musculoskeletal geometry (Abbott and Wilkie 1953; Wilkie 1956; Zajac 1989).

Torques were computed and analyzed for the shoulder and elbow joints as detailed in the equations below.

Elbow joint torques

$$\text{Interaction} = -\ddot{\theta}[A\cos(\phi) + B] - \dot{\theta}^2 A\sin(\phi)$$

$$\text{Net} = \ddot{\phi}B$$

$$\text{Muscle}_{\text{ellow}} = \text{Net} - \text{Interaction}$$

Shoulder Joint Torques

$$\text{Interaction} = -\bar{\phi}A\cos(\phi) + (\dot{\phi} + \dot{\theta})^2 A\sin(\phi)$$

$$\text{Net} = \bar{\theta}[C + \text{A}\cos(\phi)]$$

$$\text{Muscle}_{\text{shoulder}} = \text{Net} - \text{Interaction} - \text{Muscle}_{\text{elbow}}$$

Symbols

$$A = m_2 L_1 r_2 + m_{\text{d}} L_{\text{d}} r_{\text{d}}$$

$$B = I_2 + m_2 r_2^2 + I_{\text{d}} + m_{\text{d}} r_{\text{d}}^2$$

$$C = I_1 + m_1 r_1^2 + (m_2 + m_{\text{d}}) L_1^2$$

Author Manuscript Author Manuscript Author Manuscript Author Manuscript

where m is mass, r is distance to center of mass from proximal joint, L is length, I is inertia, θ is shoulder angle, and ϕ is elbow angle. The subscripts are defined as follows: 1 is upper arm segment, 2 is forearm/hand segment, and d is air sled device.

For these calculations, the aluminum rod attaching the shoulder potentiometer to the elbow potentiometer was not considered because its mass was only 0.052 kg. The inertia and mass of the forearm support were 0.0247 kgm^2 and 0.58 kg, respectively. Limb segment inertia, center of mass, and mass were computed from regression equations using subjects' body weight and measured limb segment lengths (Winter 1990).

We quantified the contributions of muscle and interaction torques to motion using the following method. Intervals during which the interaction torque component acted in the same direction as the net torque were considered to contribute to a positive interaction torque impulse. Intervals during which the interaction torque component acted in the opposite direction to net torque were considered to contribute to a negative interaction torque impulse. All positive and negative integrals were summed to yield a single total interaction torque impulse for the entire movement. Muscle torque impulse was likewise computed as a contribution to net torque for the entire movement.

Statistical analysis

The individual measures used in this paper were analyzed in separate analyses of variance (ANOVAs). Post hoc comparison of cell means was done using the Bonferoni/Dunn method. We used a simple linear regression analysis to assess the relationships between specific data sets.

RESULTS

Task learning

Final position error, hand path direction-change, and movement duration are shown in Fig. 3 for all trials, averaged across all subjects. Left and right arm data are grouped and plotted separately for comparison of performance between arms. Although movement duration remained relatively constant across the entire experimental session, movement accuracy improved during the 1st 55 trials performed with each hand, indicating task adaptation. For the following 60 trials, task accuracy remained relatively constant, as reflected by the asymptotic region of the plots (exponential fit) shown in Fig. 3. Left and right hand paths showed distinct curvatures, measured as direction-changes. The direction-changes of movements to *targets 2* and *3* were opposite for the two arms, but remained relatively constant across the duration of task performance. The direction-change measured for movements to *target 1* was also different for the two hands. Left arm movements to *target 1* showed a clockwise shift in this measure before *trial 55,* remaining relatively constant across the final 60 trials. In the following sections, we compare performance of left and right arms for the last 60 trials performed with each hand, during which movement accuracy, duration, and direction-change remained relatively constant.

Author Manuscript Author Manuscript Author Manuscript Author Manuscript

Hand kinematics

Figure 4 (*top*) shows left and right hand paths from two subjects for the 120 trials (60 for each hand) that followed task adaptation. Measures of accuracy and direction-change, averaged across all subjects, are shown below. Right and left hand paths are displayed in a "right-hand" coordinate system (see methods). The distributions in final position for the right and left hands are overlapping for *targets 2* and *3,* whereas the final positions for *target 1* showed little overlap. Both hands showed similar final position errors (distance from the target). Across all subjects, the left hand was slightly more accurate (difference of means: 2.6 ± 2.0 mm, mean ± SE; Bonferoni/Dunn: $P < 0.0043$) for *targets 2* and *3,* whereas there was no significant interlimb difference in accuracy for *target 1* (Bonferoni/Dunn: $P = 0.9201$; see Fig. 4B, right).

The most striking finding, illustrated in Fig. 4, was the difference in the trajectories taken by the right and left hands to reach the targets. For the movements directed to *targets 2* and *3,* the right hand was initially directed medial to the target, subsequently curving lateral to reach its final position, whereas left hand movements were initiated lateral to the target, subsequently curving medial. These different coordination patterns were consistent across subjects as indicated by the plot of mean direction-change (see methods) in Fig. 4B, left. Across subjects, interlimb differences in direction-change were substantial for movements to all targets (Bonferoni/Dunn: $P < 0.0001$). For movements to *target 1,* both hands showed a medial to lateral direction-change (positive value); however, the left hand paths were significantly less curved (reduced direction-change, Bonferoni/Dunn: $P < 0.0001$).

Next, we examined whether these different hand path direction-changes varied with the amount of shoulder excursion required for the different targets. As greater amounts of shoulder excursion were required by the task (*targets 1–3,* respectively), the left hand paths showed progressively greater lateral to medial direction-changes. For the left arm, the average direction-change measured for movements toward *target 1* was 3.9 ± 1.0° (mean ± SE), whereas that measured for movements to *target 3* was −22.6 ± 2.6° (difference, 26.5°; Bonferoni/Dunn: $P < 0.0001$). In contrast, the right hand paths showed slight changes in curvature that varied with direction. For movements toward *target 1,* the mean direction-change was 10.7 ± 2.0°, whereas that measured for movements to *target 3* was 13.6 ± 2.0°, a small but significant difference (2.9°, Bonferoni/Dunn: $P = 0.0033$).

Joint kinematics

Figure 5A shows representative trials made toward *target 3* by *subject 1.* The different hand path curvatures illustrated in Fig. 5A (*left*) reflect different elbow and shoulder joint coordination patterns (Fig. 5A, right). For these particular trials, the shoulder displacement profiles were almost identical. However, the elbow profiles were quite different. Although both elbows reached similar final positions, the left elbow initially extended earlier than the right elbow. As a result, left elbow excursion at peak tangential hand velocity (V_{max}) was larger. This resulted in a more lateral position of the left hand at V_{max}. Although shoulder excursions were not always identical, interlimb differences in coordinative patterns were consistent across trials, directions, and subjects. Figure 5B shows the ratio of shoulder to elbow excursion (averaged across all subjects), measured at V_{max} and at final position.

Author Manuscript Author Manuscript Author Manuscript Author Manuscript

Regardless of the target direction, the left hand showed substantially smaller excursion ratios at V_{max} (Bonferoni/Dunn: $P < 0.0001$). This indicates that for a given shoulder excursion, elbow displacement was greater for the left arm. In contrast, at the final position, right and left joint excursion ratios were not significantly different for movements made to *target 3* (Bonferoni/Dunn: $P = 0.018$) and were similar for movements made to *target 2* (left mean, 0.74 ± 0.03; right mean, 0.76 ± 0.02). Consistent with these similarities in final joint ratios, the final positions of movements made to these targets had overlapping distributions (see Fig. 3). However, for movements made toward *target 1,* right arm and left arm joint ratios remained different (Bonferoni/Dunn: $P < 0.0001$), reflecting the segregated endpoint distributions for right and left hands displayed in Fig. 4.

In summary, right and left arms showed similar accuracy in final position, however, not always with identical final configurations of the limb. Left and right hand trajectories were substantially different, with oppositely directed curvatures. These curvatures are direct indications of different interjoint coordination patterns employed by each arm. Compared to the right arm, left arm movements were systematically initiated with greater elbow extension for a given amount of shoulder flexion. The following sections examine the kinetic differences underlying these interjoint coordination patterns.

Joint kinetics

Figures 6 and 7 show representative trials made with the right and left arms, respectively, to *targets 1* and *3* by *subject 1.* Hand paths are shown at the *top,* followed by joint angle, and joint torque profiles.

In Fig. 6 (right arm) the hand paths in both directions show similar medial to lateral curvatures. As required by the task, elbow excursions are similar (24.3 and 25.0°, respectively), and shoulder excursions are different: *target 3* greater than *target 1* (6.4 and 17.2°, respectively). For both movements, shoulder motion is determined predominantly by muscle forces acting on the upper arm (interaction torque remains small relative to net torque). In contrast, interaction torques contribute substantially to elbow motion. This is evident especially during movement initiation toward *target 3* where the muscle torque counters elbow joint acceleration. Although both movements are initiated with elbow extensor acceleration, as indicated by the net torque profiles, initial muscle torque acts in opposite directions for each movement. The *target 1* movement is initiated with extensor muscle torque, whereas the *target 3* movement is initiated with flexor muscle torque.

Figure 7 (left arm, *target 1*) shows that the left hand path is nearly straight and directed lateral to *target 1*, in contrast to the corresponding right arm movement (Fig. 6, *left*). The more lateral hand trajectory results from less shoulder flexion, which is reflected by lower net shoulder torque. This is because elbow and shoulder muscle torques, acting on the upper arm, counter one another. This reduced left shoulder motion, relative to the corresponding right arm movement, results in smaller elbow joint interaction torques. Consequently, elbow joint acceleration is determined almost entirely by muscle torque. This is in contrast with the right arm movement (Fig. 6), in which interaction torques at the elbow play a larger role in the acceleration of the joint.

Author Manuscript Author Manuscript Author Manuscript Author Manuscript

Figure 7 (left arm, *target 3*) shows that the hand path is curved lateral to medial, opposite to that of the corresponding right arm movement (Fig. 6, *right*). This initial lateral deviation reflects greater left elbow extension in the early phase of motion (see RESULTS: *Joint kinematics*). During this part of the movement, shoulder net torque is similar for the two arms. However, the right arm movement is initiated with flexor elbow muscle torque (see Fig. 6, *right column*), while the left arm movement is initiated with extensor elbow muscle torque (Fig. 7, *right column*). As a result, left extensor net torque develops more rapidly, producing the early elbow joint extension that causes the initial lateral deviation in the left hand trajectory.

In summary, the examples in Figs. 6 and 7 illustrate distinct coordination strategies employed by each arm. For movements to *target 1,* right elbow and shoulder muscle torques acted synergistically to accelerate the upper arm, whereas elbow and shoulder muscle torques countered one another in accelerating the left upper arm. For both targets, interaction torques contributed more to elbow joint acceleration for the right arm than for the left arm.

Muscle and interaction torque contributions to net torque

The interlimb differences in torque strategies illustrated by the examples of Figs. 6 and 7 were consistent across all trials and all subjects. The stacked bar plots of Fig. 8 illustrate muscle and interaction torque impulse, measured as separate contributions to shoulder (left) and elbow (right) net torque (see methods). For this analysis, interaction torque impulse is considered positive when the interaction torque acts in the same direction (flexor or extensor) as the joint's net torque. Muscle torque impulse was computed in the same way (see methods). The mean ± SE, calculated across all trials for each subject, is plotted for each arm and target direction in Fig. 8. (Note: net joint torque is equal to the summed positive and negative bar plot height.)

In general, right and left elbow joint *net* torques were similar, whereas right shoulder net torque was greater than left shoulder net torque. It should be noted that elbow net torque varies with elbow joint acceleration, whereas shoulder net torque varies with shoulder acceleration and elbow angle. Because left and right elbow displacements were different for movements to the same targets, differences in net shoulder joint torque values do not directly indicate differences in shoulder joint acceleration.

As expected by the design of the task (same net elbow excursion required for all targets), elbow net torque impulse was similar across all three target directions for both hands (all subjects: *target 1,* 0.61 ± 0.16 Nms, mean ± SD; *target 2,* 0.66 ± 0.14 Nms; *target 3,* 0.58 ± 0.15 Nms). In contrast, shoulder net torque impulse increased substantially across the three target directions, as successively more net shoulder joint excursion was required for targets two and three, respectively (all subjects, both arms: *target 1,* 0.260 ± 0.15 Nms, mean ± SD; *target 2,* 0.695 ± 0.16 Nms; *target 3,* 0.954 ± 0.22 Nms). The percentage change in mean net shoulder torque impulse for movements to *target 3* compared with that for movements to *target 1* was 267%, whereas the corresponding change in mean net elbow torque impulse was −4.9%. Furthermore, as greater shoulder motion was required by the task, the contributions of elbow interaction torque to elbow net torque increased substantially. For both hands, the mean elbow joint interaction torque impulses were 0.179

Author Manuscript Author Manuscript Author Manuscript Author Manuscript

± 0.087 (SD) Nms for *target 1,* 0.337 ± 0.101 Nms for *target 2,* and 0.461 ± 0.127 Nms for *target 3.* Thus mean elbow interaction torque impulse increased 2.5-fold for *target 3* movements, compared with *target 1* movements.

Regardless of the target, the contributions of elbow joint interaction torque impulse to net torque impulse was almost 20% greater for right arm movements, as compared with left arm movements (see Table 1 and Fig. 8). Elbow muscle torque, thus contributed substantially less toward acceleration of the right elbow, compared with acceleration of the left elbow, for movements to all three directions (Bonferoni/Dunn: $P < 0.0001$). For *target 3* movements, in which elbow joint interaction torques were largest, right elbow muscle torque impulse contributed <7% to elbow net torque impulse, whereas left elbow muscle torque impulse contributed almost 30% to elbow net torque impulse. Thus for this direction, right elbow acceleration was determined almost entirely by interaction torque, whereas left elbow muscle torque contributed substantially more to acceleration of the left elbow joint (see Table 1). In summary, the right arm coordination strategy more extensively employed muscle torque at the shoulder to accelerate the elbow, indicating more effective utilization of interaction torques.

Left elbow muscle torque not only contributed greater to elbow joint acceleration, but also to shoulder joint acceleration. It should be noted that muscles crossing the elbow joint produce equal and opposite forces on the distal upper arm and the proximal forearm. Thus elbow muscle torque directly affects both elbow and shoulder joint acceleration. For all directions, left elbow muscle torque impulse contributed greater than twice as much to shoulder joint net torque impulse than did right elbow muscle torque impulse (Bonferoni/Dunn: $P < 0.0001$; see Table 2 and Fig. 8). Thus for the left arm, elbow joint muscle torque contributed greater to motion at both joints. In contrast, for the right arm, elbow and shoulder joint acceleration was determined to a greater extent by shoulder muscle torque.

Dependence of hand path direction-changes on intersegmental dynamics

We examined the extent to which the hand path direction-changes, made by the right and left arms, were dependent on interaction torque impulse. Figure 9 shows sample scatter plots of our measure of hand path direction-change plotted against interaction torque impulse (calculated across the entire movement, as a contribution to net torque) from *subject 1* data (*left*), and regression coefficients for all subject data (*right*). For all subjects, left hand direction-change was highly dependent on interaction torque impulse. However, variation in right hand direction-change could not be accounted for by variation in interaction torque impulse. Thus right arm hand path shape was independent of direction-dependent variations in interaction torques, whereas left arm hand path shape varied directly with interaction torques. This is consistent with the fact that the left hand path direction-changes varied with target direction, becoming greater as more shoulder excursion was required by the target, whereas the right hand path direction-changes did not (see Fig. 4). We reasoned that the right arm controller must have accounted for interaction forces, to specify muscle actions that combine with these forces such that the shape of the hand path was not dependent on their magnitude. Such independence of hand path shape from direction-dependent variations in interaction torque implies greater control of the hand trajectory for the dominant arm.

Author Manuscript Author Manuscript Author Manuscript Author Manuscript

DISCUSSION

This study examined the coordination patterns employed for the left and right arms during rapid targeted reaching movements made by right-handed subjects. Movements were made to each of three targets, designed to elicit progressively greater amplitude interaction torques at the elbow joint. Subjects received visual feedback only of the final hand position with respect to the target location, whereas points were awarded based on final position accuracy for movements made within an interval of 400–600 ms. For all subjects, the right and left hands showed a similar time course of improvement in final position accuracy over repeated trials. After task adaptation, final position accuracy was similar for both hands; however, the hand trajectories and joint coordination patterns during the movement were systematically different. The trajectories of both hands were not straight but exhibited oppositely directed curvatures. Right hand paths showed similar medial to lateral curvatures for all target directions. The left hand paths had lateral to medial curvatures, which increased in magnitude as greater shoulder excursions were required.

Kinetic analysis revealed differences in the control strategies employed for the left and right arms. For movements requiring substantial shoulder excursions (*targets 2* and *3*), right arm coordination was characterized by a control strategy, in which movement of both joints was primarily driven by the effects of shoulder muscle actions. In contrast, motion of the left elbow and shoulder joints was substantially effected by elbow muscles through direct actions on the upper arm and forearm segments. In other words, interaction torques contributed more to the acceleration of the right elbow than the left elbow. Furthermore, the direction-changes (curvatures) of the right hand paths were independent, whereas those of the left hand paths were dependent, on variations in elbow joint interaction torque impulse.

Right (dominant) arm control

Our findings for the right arm are consistent with previous reports that demonstrated that adaptation to task-specific dynamics occurs through the development of internal representations of the applied loads. During practice under particular viscous, coriolis, and inertial loading conditions (Gandolfo et al. 1996; Goodbody and Wolpert 1998; Lackner and Dizio 1994; Sainburg et al. 1999; Shadmehr and Mussa-Ivaldi 1994), the CNS develops internal models of the applied forces that are used to predict musculoskeletal and environmental dynamics for planning subsequent movements. In the current study, the independence of dominant hand path shape from interaction torque indicates skillful coordination of muscle actions with intersegmental dynamics and indicates accurate predictions of those interactions. For example, during *target 3* movements, extension of the right elbow was initiated with flexor, or near zero, elbow muscle torque, exemplifying the anticipation of extensor interaction torque before movement initiation (see Fig. 6, *target 3*). Such predictions are requisite to achieving variable control over the hand trajectory under different task conditions. In contrast, nondominant hand path shape deviated directly with interaction torque amplitude, indicating less accurate predictions of those interactions. Consistent with this finding, Hore et al. (1996) recently demonstrated that dominant arm advantages in throwing accuracy are related to more consistent timing of finger extension relative to proximal limb motion, indicating interlimb differences in the coordination of

Author Manuscript Author Manuscript Author Manuscript Author Manuscript

proximal and distal joints. Our findings extend those of Hore, suggesting that dominant arm advantages for interjoint coordination result from more accurate predictions of the effects of intersegmental dynamics during movement planning. Our results are thus consistent with the anecdotal observation that the dominant arm can achieve more varied and flexible control over movement trajectories, as required for accurate drawing, writing, and ball throwing.

Left (nondominant) arm control

It appears contradictory that the two limbs achieved similar final position accuracy, whereas the left arm demonstrated less effective control of intersegmental dynamics. However, it has previously been proposed that control of limb trajectory and posture is implemented by distinct mechanisms (Gottlieb 1996; Hirayama et al. 1993). Hirayama demonstrated the plausibility of such control using a two-phase model to implement a simulation, in which movement was initiated through a forward dynamic controller (open-looped), whereas final position was achieved by increasing joint stiffness about an equilibrium posture (coactivation of antagonist muscles). Gottlieb (1996) elaborated a similar, three-element model, in which each component of control can be differentially weighted depending on the current demands of the task. According to this model, initial trajectory features result from open-loop mechanisms (α), based on internal representations of task dynamics. The second element (λ) defines feedback mediated control, largely effecting limb compliance. The third element (γ) describes active modulation of the feedback elements. If task dynamics are incompletely or incorrectly modeled by the controller, the effects of feedback can be amplified by way of the γ command, thereby increasing joint viscosity as well as stiffness about a desired trajectory. This will reduce potential path deviations due to inaccurate predictions of impending mechanical interactions. In this particular case, control would mimic that described by the equilibrium point hypotheses, because joint torque will emerge largely as a function of the difference between the muscle lengths for the current and the desired limb positions (Bizzi 1987; Bizzi and Abend 1983; Bizzi et al. 1976, 1982; Feldman 1986; Flash 1987; Polit and Bizzi 1979). Under such conditions, the trajectory would be expected to deviate with task-specific inertial dynamics, such as interaction torques. As the limb slows down and approaches the final position, the λ command becomes dominant, and feedback-mediated increases in joint stiffness and viscosity substantially reduce potential path deviations and errors in final position. This type of mechanism may explain the behavior of the nondominant arm in the current study for which trajectory deviations, but not final position errors, varied with the magnitude of interaction torques.

Distinct neural mechanisms for right and left arm movements

The distinct coordination patterns observed for the left and right arms are not likely to have resulted from differences in peripheral factors, such as muscle strength or distribution of muscle fiber types. Such differences would be expected to alter the rate of change of muscle force generation (Burke 1981; Enoka 1988). However, our results show interlimb differences in the relative timing, magnitude, and direction of muscle torques at the shoulder and elbow that are more likely to result from differences in neural activation. For example, substantial differences in the direction of muscle torque occurred at movement initiation. *Target 1* movements were consistently initiated with extensor muscle torque at the left

Author Manuscript Author Manuscript Author Manuscript Author Manuscript

shoulder, but with flexor muscle torque at the right shoulder (see Figs. 6–8). Similarly, for *target 3* movements, right elbow extension was initiated with flexor (or near zero) elbow muscle torque, whereas left elbow extension was initiated with substantial extensor muscle torque (see Figs. 6–8). Furthermore, the magnitude of the left shoulder muscle torque was less than that of the right shoulder, whereas the magnitude of the left elbow muscle torque was larger than that of the right elbow (see Figs. 6–8). Strength differences between the arms could not account for such muscle torque patterns. Instead, such differences in muscle joint torque must result from interlimb differences in patterns of neural activation of muscles.

The hypothesis that control of the two limbs is mediated by distinct neural mechanisms is consistent with previous work indicating different neural contributions to unilateral movements of right and left arms. The landmark studies by Kuypers and colleagues established that, although trunk and limb girdle musculatures are controlled through bilateral projections, control of arm musculature for reach and prehension arises primarily from contralateral cortex, either directly through descending corticospinal projections, or indirectly through brain stem pathways (Holstege and Kuypers 1982, 1987; Kuypers 1982; Kuypers and Brinkman 1970; Kuypers and Laurence 1967; Kuypers and Maisky 1975; Kuypers et al. 1962; Lawrence and Kuypers 1968a,b). Subsequent electrophysiological and neural imaging studies have revealed substantial activation of ipsilateral motor cortex during unimanual arm and finger movements (Chen et al. 1997a,b; Dassonville et al. 1997; Gitelman et al. 1996; Kawashima et al. 1994, 1996–1998; Kim et al. 1993; Kutas and Donchin 1974; Macdonell et al. 1991; Matsunami and Hamada 1981; Salmelin et al. 1995; Taniguchi et al. 1998; Tanji et al. 1988; Urbano et al. 1996; Viviani et al. 1998; Volkmann et al. 1998). However, activation of left and right hemispheres during unilateral upper limb movements are not symmetrical for movements of the dominant and nondominant arms (Amunts et al. 1996; Dassonville et al. 1997; Gitelman et al. 1996; Kawashima et al. 1997; Kim et al. 1993; Taniguchi et al. 1998; Tanji et al. 1988; Urbano et al. 1996; Viviani et al. 1998; Volkmann et al. 1998). Furthermore, handedness has been associated with morphological asymmetries in motor cortex, basal ganglia, and cerebellum (Amunts et al. 1996; Kooistra and Heilman 1988; Snyder et al. 1995). Such physiological and morphological asymmetries are consistent with the idea that voluntary movement of the two arms is achieved through independent controllers.

The differences in coordination between the limbs reported in this study may reflect the more extensive, lifelong, practice and experience that is often associated with dominant limb use. This hypothesis is supported by previous reports indicating that accurate coordination of muscle forces with intersegmental and environmental forces is dependent on proprioceptive information (Ghez and Sainburg 1995; Sainburg et al. 1993, 1995) and learning (Lackner and Dizio 1994; Sainburg et al. 1999; Shadmehr and Mussa-Ivaldi 1994), and that such coordination develops over the first few years of life (Thelen et al. 1983, 1993; Zernicke and Schneider 1993). Alternatively, it has been proposed that the behavioral effects of handedness are determined by physiological asymmetries that are present before the opportunity for such experience develops (Annett 1992; Clark et al. 1996; Coryell 1985; Drea et al. 1995; McManus 1985; Melsbach et al. 1996; Tan 1990). According to this idea, handedness emerges from unique neural circuits in each hemisphere that are specialized for controlling different aspects of limb movements. This hypothesis is supported by evidence

Author Manuscript Author Manuscript Author Manuscript Author Manuscript

of handedness in human fetuses and newborns (Caplan and Kinsbourne 1976; Coryell 1985; Futagi et al. 1995; Hepper et al. 1998, 1991; Konishi et al. 1986, 1997; Ottaviano et al. 1989; Tan et al. 1992). At present, however, there is insufficient data to distinguish between these alternatives.

Acknowledgments

The authors thank G. Johnson, Columbia University College of Physicians and Surgeons, for design of the air jets used in this study. Fabrication of these air jets was done by One of A Kind Ltd., Lincoln Park, NJ.

This research was supported by National Institute of Child Health and Human Development Grants 1k01HD-0118601 and T32HD-07423.

REFERENCES

Abbott BC and Wilkie PR The relation between velocity of shortening and tension-length curve of skeletal muscle. J. Physiol. (Lond.) 120: 214–223, 1953. [PubMed: 13062233]

Amunts K, Schlaug G, Schleicher A, Steinmetz H, Dabringhaus A, Roland PE, and Zilles K Asymmetry in the human motor cortex and handedness. Neuroimage 4: 216–222, 1996. [PubMed: 9345512]

Annett J, Annett M, and Hudson PTW The control of movement in the preferred and non-preferred hands. Q. J. Exp. Psychol. B 31: 641–652, 1979.

Annett M Parallels between asymmetries of Planum temporale and of hand skill. Neuropsychologia 30: 951–962, 1992. [PubMed: 1470339]

Bizzi E Motor control mechanisms. An overview. Neurologic Clinics 5: 523–528, 1987. [PubMed: 3431534]

Bizzi E and Abend W Posture control and trajectory formation in single- and multi-joint arm movements. Adv. Neurol. 39: 31–45, 1983. [PubMed: 6419552]

Bizzi E, Accornero N, Chapple W, and Hogan N Arm trajectory formation in monkeys. Exp. Brain Res. 46: 139–143, 1982. [PubMed: 6802666]

Bizzi E, Polit A, and Morasso P Mechanisms underlying achievement of final head position. J. Neurophysiol. 39: 435–444, 1976. [PubMed: 815518]

Burke RE Motor units. Anatomy, physiology, and functional organization. In: Handbook of Physiology. The Nervous System. Motor Control. Bethesda, MD: Am. Physiol. Soc., 1981, sect. 1, vol. II, p. 345–422.

Caplan PJ and Kinsbourne M Baby drops the rattle: asymmetry of duration of grasp by infants. Child Dev. 47: 532–534, 1976. [PubMed: 1269321]

Carson RG Visual feedback processing and manual asymmetries: an evolving perspective. In: Vision and Motor Control. Advances in Psychology, edited by Proteau L and Elliott D. Amsterdam: North-Holland, 1992, p. 49–65.

Carson RG, Chua R, Elliott D, and Goodman D The contribution of vision to asymmetries in manual aiming. Neuropsychologia 28: 1215–1220, 1990. [PubMed: 2290495]

Carson RG, Chua R, Goodman D, Byblow WD, and Elliott D The preparation of aiming movements. Brain Cogn. 28: 133–154, 1995. [PubMed: 7546669]

Carson RG, Goodman D, Chua R, and Elliott D Asymmetries in the regulation of visually guided aiming. J. Mot. Behav. 25: 21–32, 1993. [PubMed: 12730038]

Chen R, Cohen LG, and Hallett M Role of the ipsilateral motor cortex in voluntary movement. Can. J. Neurol. Sci. 24: 284–291, 1997a. [PubMed: 9398974]

Chen R, Gerloff C, Hallett M, and Cohen LG Involvement of the ipsilateral motor cortex in finger movements of different complexities. Ann. Neurol. 41: 247–254, 1997b. [PubMed: 9029074]

Clark MM, Robertson RK, and Galef BG Jr. Effects of perinatal testosterone on handedness of gerbils: support for part of the Geschwind-Galaburda hypothesis. Behav. Neurosci. 110: 413–417, 1996. [PubMed: 8731067]

Author Manuscript Author Manuscript Author Manuscript Author Manuscript

Coryell J Infant rightward asymmetries predict right-handedness in childhood. Neuropsychologia 23: 269–271, 1985. [PubMed: 4000462]

Dassonville P, Zhu XH, Uurbil K, Kim SG, and Ashe J Functional activation in motor cortex reflects the direction and the degree of handedness. Proc. Natl. Acad. Sci. USA 94: 14015–14018, 1997. [PubMed: 9391144]

Drea CM, Wallen K, Akinbami MA, and Mann DR Neonatal testosterone and handedness in yearling rhesus monkeys (Macaca mulatta). Physiol. Behav. 58: 1257–1262, 1995. [PubMed: 8623029]

Elliott D, Chua R and Pollock BJ The influence of intermittent vision on manual aiming. Acta Psychol. 85: 1–13, 1994.

Elliott D, Roy EA, Goodman D, Carson RG, Chua R, and Maraj BKV Asymmetries in the preparation and control of manual aiming movements. Can. J. Exp. Psychol. 47: 570–589, 1993.

Enoka RM Muscle strength and its development: new perspectives. Sports Med. 6: 146–168, 1988. [PubMed: 3055145]

Feldman A Once more on the equilibrium point hypothesis (h model) for motor control. J. Mot. Behav. 19: 749–753, 1986.

Flash T The control of hand equilibrium trajectories in multi-joint arm movements. Biol. Cybern. 57: 257–274, 1987. [PubMed: 3689835]

Flowers K Handedness and controlled movement. Br. J. Psychol. 66: 39–52, 1975. [PubMed: 1131479]

Futagi Y, Otani K, and Imai K Asymmetry in plantar grasp response during infancy. Pediatr. Neurol. 12: 54–57, 1995. [PubMed: 7748362]

Gandolfo F, Mussa-Ivaldi FA, and Bizzi E Motor learning by field approximation. Proc. Natl. Acad. Sci. USA 93: 3843–3846, 1996. [PubMed: 8632977]

Ghez C and Sainburg R Proprioceptive control of interjoint coordination. Can. J. Physiol. Pharmacol. 73: 273–284, 1995. [PubMed: 7621366]

Gitelman DR, Alpert NM, Kosslyn S, Daffner K, Scinto L, Thompson W, and Mesulam MM Functional imaging of human right hemispheric activation for exploratory movements. Ann. Neurol. 39: 174–179, 1996. [PubMed: 8967748]

Goodbody SJ and Wolpert DM Temporal and amplitude generalization in motor learning. J. Neurophysiol. 79: 1825–1838, 1998. [PubMed: 9535951]

Gottlieb GL On the voluntary movement of compliant (inertial-viscoelastic) loads by parcellated control mechanisms. J. Neurophysiol. 76: 3207–3229, 1996. [PubMed: 8930267]

Hepper PG, Mccartney GR, and Shannon EA Lateralised behaviour in first trimester human foetuses. Neuropsychologia 36: 531–534, 1998. [PubMed: 9705063]

Hepper PG, Shahidullah S, and White R Handedness in the human fetus. Neuropsychologia 29: 1107–1111, 1991. [PubMed: 1775228]

Hirayama M, Kawato M, and Jordan MI The cascade neural network model and a speed-accuracy trade-off of arm movement. J. Mot. Behav. 25: 162–174, 1993. [PubMed: 12581987]

Holstege G and Kuypers HG The anatomy of brain stem pathways to the spinal cord in cat. A labeled amino acid tracing study. Prog. Brain Res. 57: 145–175, 1982. [PubMed: 7156396]

Holstege JC and Kuypers HG Brainstem projections to lumbar motoneurons in rat. I. An ultrastructural study using autoradiography and the combination of autoradiography and horseradish peroxidase histochemistry. Neuroscience 21: 345–367, 1987. [PubMed: 3614638]

Hore J, Watts S, Tweed D, and Miller B Overarm throws with the nondominant arm: kinematics of accuracy. J. Neurophysiol. 76: 3693–3704, 1996. [PubMed: 8985867]

Kawashima R, Inoue K, Sato K, and Fukuda H Functional asymmetry of cortical motor control in left-handed subjects. Neuroreport 8: 1729–1732, 1997. [PubMed: 9189922]

Kawashima R, Itoh H, Ono S, Satoh K, Furumoto S, Gotoh R, Koyama M, Yoshioka S, Takahashi T, Takahashi K, Yanagisawa T, and Fukuda H Changes in regional cerebral blood flow during self-paced arm and finger movements. A PET study. Brain Res. 716: 141–148, 1996. [PubMed: 8738230]

Kawashima R, Matsumura M, Sadato N, Naito E, Waki A, Nakamura S, Matsunami K, Fukuda H, and Yonekura Y Regional cerebral blood flow changes in human brain related to ipsilateral and

Author Manuscript Author Manuscript Author Manuscript Author Manuscript

contralateral complex hand movements–a PET study. Eur. J. Neurosci. 10: 2254–2260, 1998. [PubMed: 9749754]

Kawashima R, Roland PE, and O'Sullivan BT Activity in the human primary motor cortex related to ipsilateral hand movements. Brain Res. 663: 251–256, 1994. [PubMed: 7874508]

Kim SG, Ashe J, Hendrich K, Ellermann JM, Merkle H, Ugurbil K, and Georgopoulos AP Functional magnetic resonance imaging of motor cortex: hemispheric asymmetry and handedness. Science 261: 615–617, 1993. [PubMed: 8342027]

Konishi Y, Mikawa H, and Suzuki J Asymmetrical head-turning of preterm infants: some effects on later postural and functional lateralities. Dev. Med. Child Neurol. 28: 450–457, 1986. [PubMed: 3758498]

Konishi Y, Takaya R, Kimura K, Takeuchi K, Saito M, and Konishi K Laterality of finger movements in preterm infants. Dev. Med. Child Neurol. 39: 248–252, 1997. [PubMed: 9183264]

Kooistra CA and Heilman KM Motor dominance and lateral asymmetry of the globus pallidus. Neurology 38: 388–390, 1988. [PubMed: 3347342]

Kutas M and Donchin E Studies of squeezing: handedness, responding hand, response force, and asymmetry of readiness potential. Science 186: 545–548, 1974. [PubMed: 4469679]

Kuypers HG A new look at the organization of the motor system. Prog. Brain Res. 57: 381–403, 1982. [PubMed: 6818612]

Kuypers HGHM and Brinkman J Precentral projections to different parts of the spinal intermediate zone in the rhesus monkey. Brain Res. 24: 29–48, 1970. [PubMed: 4099987]

Kuypers HGJM and Laurence DG Cortical projections to the red nucleus and the brain stem in the rhesus monkey. Brain Res. 4: 151–188, 1967. [PubMed: 4961812]

Kuypers HGMJ, Fleming WR, and Farinholt JW Subcorticospinal projections in the rhesus monkey. J. Comp. Neurol. 118: 107–137, 1962. [PubMed: 14461005]

Kuypers HGMJ and Maisky VA Retrograde axonal transport of horseradish peroxidase from spinal cord to brain stem cell groups in the cat. Neurosci. Lett. 1: 9–14, 1975. [PubMed: 19604744]

Lackner JR and Dizio P Rapid adaptation to Coriolis force perturbations of arm trajectory. J. Neurophysiol. 72: 299–313, 1994. [PubMed: 7965013]

Lawrence DG and Kuypers HG The functional organization of the motor system in the monkey. I. The effects of bilateral pyramidal lesions. Brain 91: 1–14, 1968a. [PubMed: 4966862]

Lawrence DG and Kuypers HG The functional organization of the motor system in the monkey. II. The effects of lesions of the descending brain-stem pathways. Brain 91: 15–36, 1968b. [PubMed: 4966860]

Macdonell RA, Shapiro BE, Chiappa KH, Helmers SL, Cros D, Day BJ, and Shahani BT Hemispheric threshold differences for motor evoked potentials produced by magnetic coil stimulation. Neurology 41: 1441–1444, 1991. [PubMed: 1891095]

Matsunami K and Hamada I Characteristics of the ipsilateral movement-related neuron in the motor cortex of the monkey. Brain Res. 204: 29–42, 1981. [PubMed: 7248755]

Mcmanus IC Handedness, language dominance and aphasia: a genetic model. Psychol. Med.-Monograph Suppl. 8: 1–40, 1985.

Melsbach G, Wohlschlager A, Spiess M, and Gunturkun O Morpho-logical asymmetries of motoneurons innervating upper extremities: clues to the anatomical foundations of handedness? Int. J. Neurosci. 86: 217–224, 1996. [PubMed: 8884392]

Oldfield RC The assessment and analysis of handedness: the Edinburgh Inventory. Neuropsychologia 9: 97–113, 1971. [PubMed: 5146491]

Ottaviano S, Guidetti V, Allemand F, Spinetoli B, and Seri SLaterality of arm movement in full-term newborn. Early Hum. Dev. 19: 3–7, 1989. [PubMed: 2721420]

Polit A and Bizzi E. Characteristics of motor programs underlying arm movements in monkeys. J. Neurophysiol. 42: 183–194, 1979. [PubMed: 107279]

Roy EA and Elliott D Manual asymmetries in visually directed aiming. Can. J. Psychol. 40: 109–121, 1986. [PubMed: 3730950]

Sainburg RL, Ghez C, and Kalakanis D Intersegmental dynamics are controlled by sequential anticipatory, error correction, and postural mechanisms. J. Neurophysiol. 81: 1040–1056, 1999.

Author Manuscript Author Manuscript Author Manuscript Author Manuscript

Sainburg RL, Ghilardi MF, Poizner H, and Ghez C Control of limb dynamics in normal subjects and patients without proprioception. J. Neurophysiol. 73: 820–835, 1995. [PubMed: 7760137]

Sainburg RL, Poizner H, and Ghez C Loss of proprioception produces deficits in interjoint coordination. J. Neurophysiol. 70: 2136–2147, 1993. [PubMed: 8294975]

Salmelin R, Forss N, Knuutila J, and Hari R Bilateral activation of the human somatomotor cortex by distal hand movements. Electroencephalogr. Clin. Neurophysiol. 95: 444–452, 1995. [PubMed: 8536573]

Shadmehr R and Mussa-Ivaldi FA Adaptive representation of dynamics during learning of a motor task. J. Neurosci. 14: 3208–3224, 1994. [PubMed: 8182467]

Snyder PJ, Bilder RM, Wu H, Bogerts B, and Lieberman JA Cerebellar volume asymmetries are related to handedness: a quantitative MRI study. Neuropsychologia 33: 407–419, 1995. [PubMed: 7617152]

Steingruber HS Handedness as a function of test complexity. Percept. Mot. Skills 40: 263–266, 1975. [PubMed: 1167961]

Tan U The left brain determines the degree of left-handedness. Int. J. Neurosci. 53: 75–85, 1990. [PubMed: 2265951]

Tan U, Ors R, Kurkcuoglu M, Kutlu N, and Cankaya A Lateralization of the grasp reflex in male and female human newborns. Int. J. Neurosci. 62: 155–163, 1992. [PubMed: 1305603]

Taniguchi M, Yoshimine T, Cheyne D, Kato A, Kihara T, Ninomiya H, Hirata M, Hirabuki N, Nakamura H, and Hayakawa T Neuromagnetic fields preceding unilateral movements in dextrals and sinistrals. Neuroreport 9: 1497–1502, 1998. [PubMed: 9631455]

Tanji J, Okano K, and Sato KC Neuronal activity in cortical motor areas related to ipsilateral, contralateral, and bilateral digit movements of the monkey. J. Neurophysiol. 60: 325–343, 1988. [PubMed: 3404223]

Thelen E, Corbetta D, Kamm K, Spencer JP, Schneider K, and Zernicke RF The transition to reaching: mapping intention and intrinsic dynamics. Child Dev. 64: 1058–1098, 1993. [PubMed: 8404257]

Thelen E, Ridley-Johnson R, and Fisher DM Shifting patterns of bilateral coordination and lateral dominance in the leg movements of young infants. Dev. Psychobiol. 16: 29–46, 1983. [PubMed: 6825965]

Todor JI and Cisneros J Accommodation to increased accuracy demands by the right and left hands. J. Mot. Behav. 17: 355–372, 1985. [PubMed: 15140687]

Urbano A, Babiloni C, Onorati P, and Babiloni F Human cortical activity related to unilateral movements. A high resolution EEG study. Neuroreport 8: 203–206, 1996. [PubMed: 9051781]

Viviani P, Perani D, Grassi F, Bettinardi V, and Fazio F Hemispheric asymmetries and bimanual asynchrony in left- and right-handers. Exp. Brain Res. 120: 531–536, 1998. [PubMed: 9655240]

Volkmann J, Schnitzler A, Witte OW, and Freund H Handedness and asymmetry of hand representation in human motor cortex. J. Neurophysiol. 79: 2149–2154, 1998. [PubMed: 9535974]

Wilkie DR The mechanical properties of muscle. Br. Med. Bull. 12: 177–182, 1956. [PubMed: 13364297]

Winter DA Biomechanics and Motor Control of Human Movement. New York: Wiley, 1990.

Zajac FE Muscle and tendon: properties, models, scaling and application to biomechanics and motor control. In: CRC Critical Reviews in Biomedical Engineering (4th ed.), edited by Bourne JR. Boca Raton, FL: CRC, 1989, p. 359–411.

Zajac FE and Gordon ME Determining muscle's force and action in multi-articular movement. Exerc. Sport Sci. Rev. 17: 187–230, 1989. [PubMed: 2676547]

Zernicke RF and Schneider K Biomechanics and developmental neuromotor control. Child Dev. 64: 982–1004, 1993. [PubMed: 8404272]

Author Manuscript Author Manuscript Author Manuscript Author Manuscript

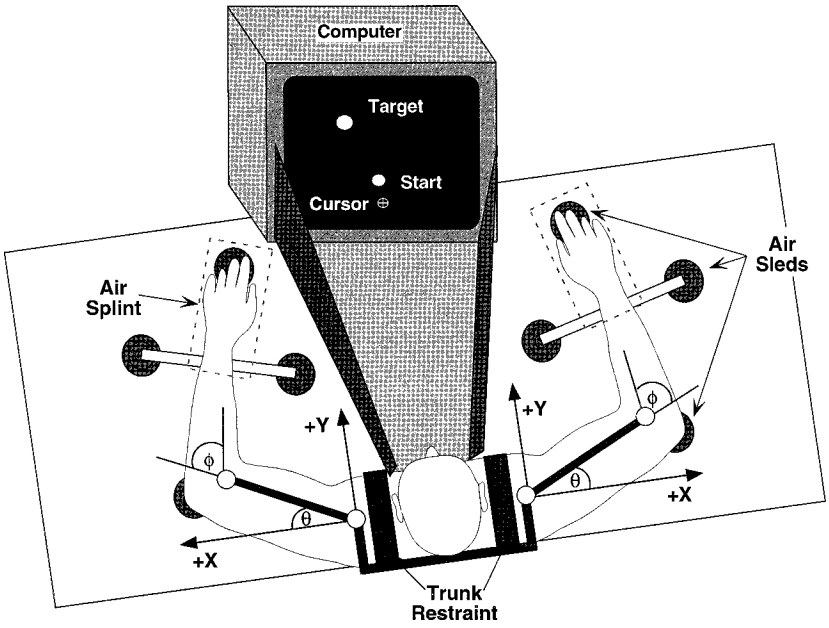

FIG. 1.

Experimental setup: X and Y represent axes of coordinate system originating at shoulder. Shoulder and elbow angles were measured as θ and ϕ, respectively. The trunk and scapulae were restrained with a butterfly style chest brace, whereas wrist and fingers were immobilized by air splints. Vision of the table and arms was blocked during the experimental sessions.

Author Manuscript Author Manuscript Author Manuscript Author Manuscript

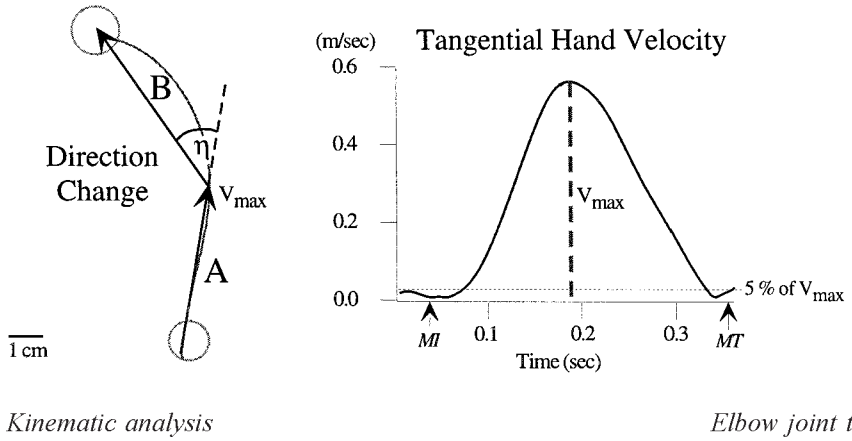

FIG. 2.

Hand path "direction-change" was quantified as the angle (η) between the 2 vectors drawn over the hand path (*left*). Vector A starts at movement initiation (MI) and ends at the point corresponding to maximum tangential hand velocity (V_{max}), identified on the tangential hand velocity plot (*right*). Vector B begins at V_{max} and ends at movement termination (MT).

Author Manuscript
Author Manuscript
Author Manuscript
Author Manuscript

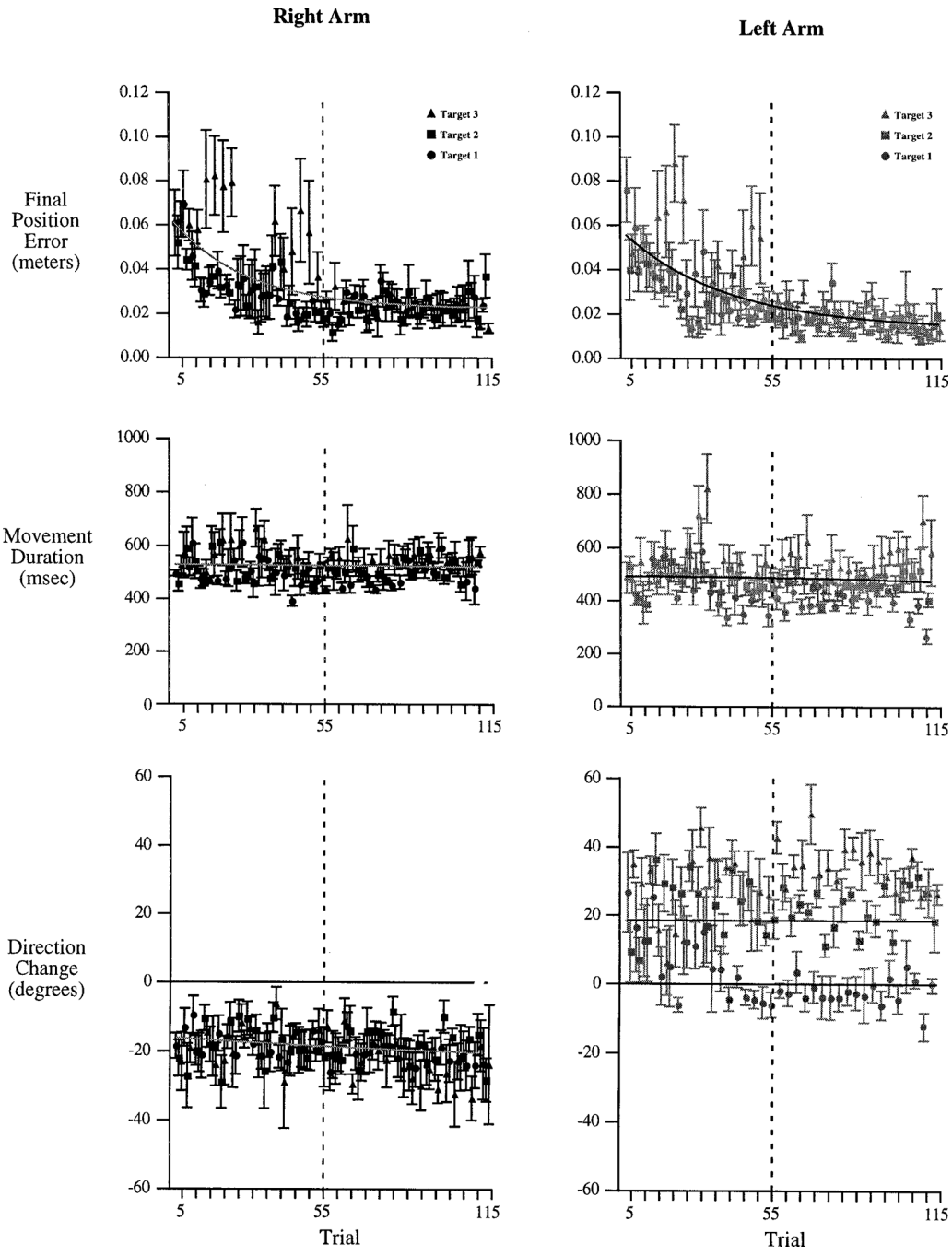

FIG. 3.

Measures of final position error (*top*), movement duration (*middle*) and direction-change (*bottom*). Each point represents a single trial, averaged across all 6 subjects. Trials for right (black) and left (gray) arms have been separated for comparison. The *x*-axis represents intralimb trial number.

Author Manuscript Author Manuscript Author Manuscript Author Manuscript

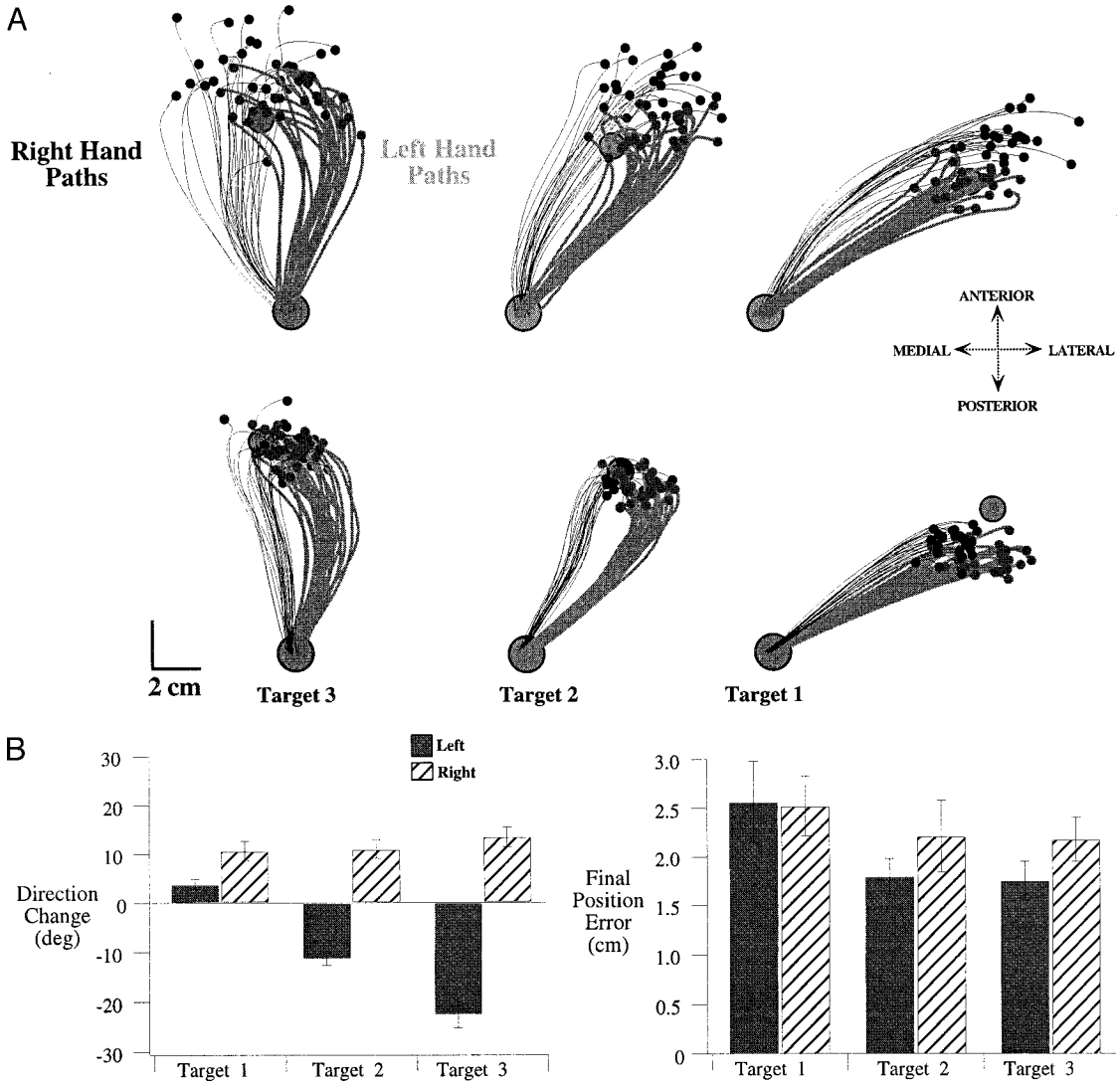

FIG. 4.

A: hand paths for all trials of *subject 1* (*top*) and *subject 2* (*bottom*). Both right hand (thin, black) and left hand (thick, gray) paths are plotted in a "right hand" coordinate system, with the medial to lateral dimension plotted along the negative to positive *x*-axis. *B*: mean ± SE for measures of direction-change (*left*) and final position error (*right*). Values are averages of the individual subject means for each measure, taken separately for each limb and each target.

Author Manuscript Author Manuscript Author Manuscript Author Manuscript

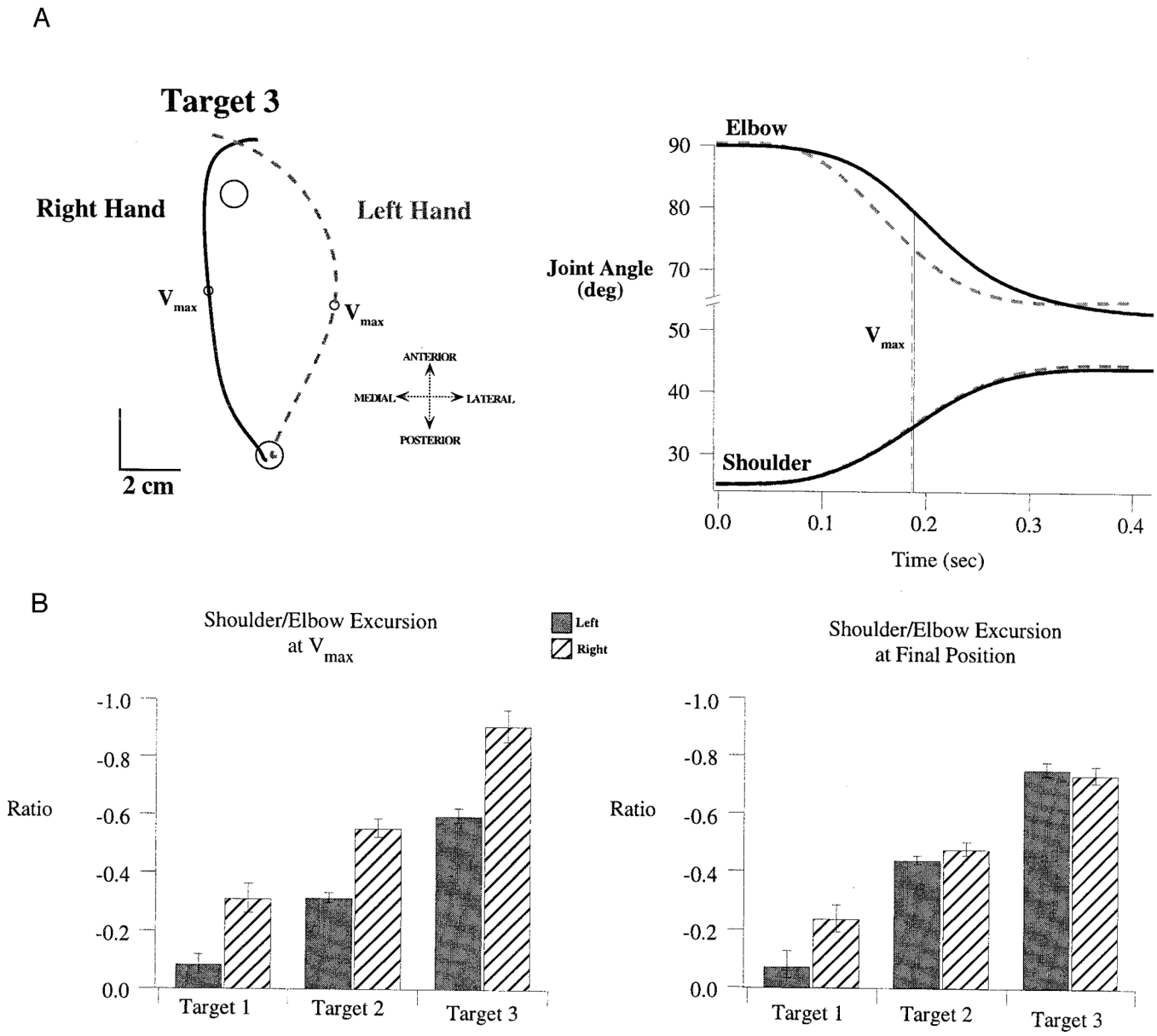

FIG. 5.

A: sample trials performed with right arm (black, solid) and left arm (gray, dashed) to *target 3.* Hand paths (*left*) are plotted in a "right hand" coordinate system, and joint displacement profiles are shown to the *right* of these. *B*: mean ± SE for measures of the shoulder excursion/elbow excursion ratio, measured at V_{max} (*left*) and at final position (*right*). Values are averages of the individual subject means for each measure, taken separately for each limb and each target.

Author Manuscript Author Manuscript Author Manuscript Author Manuscript

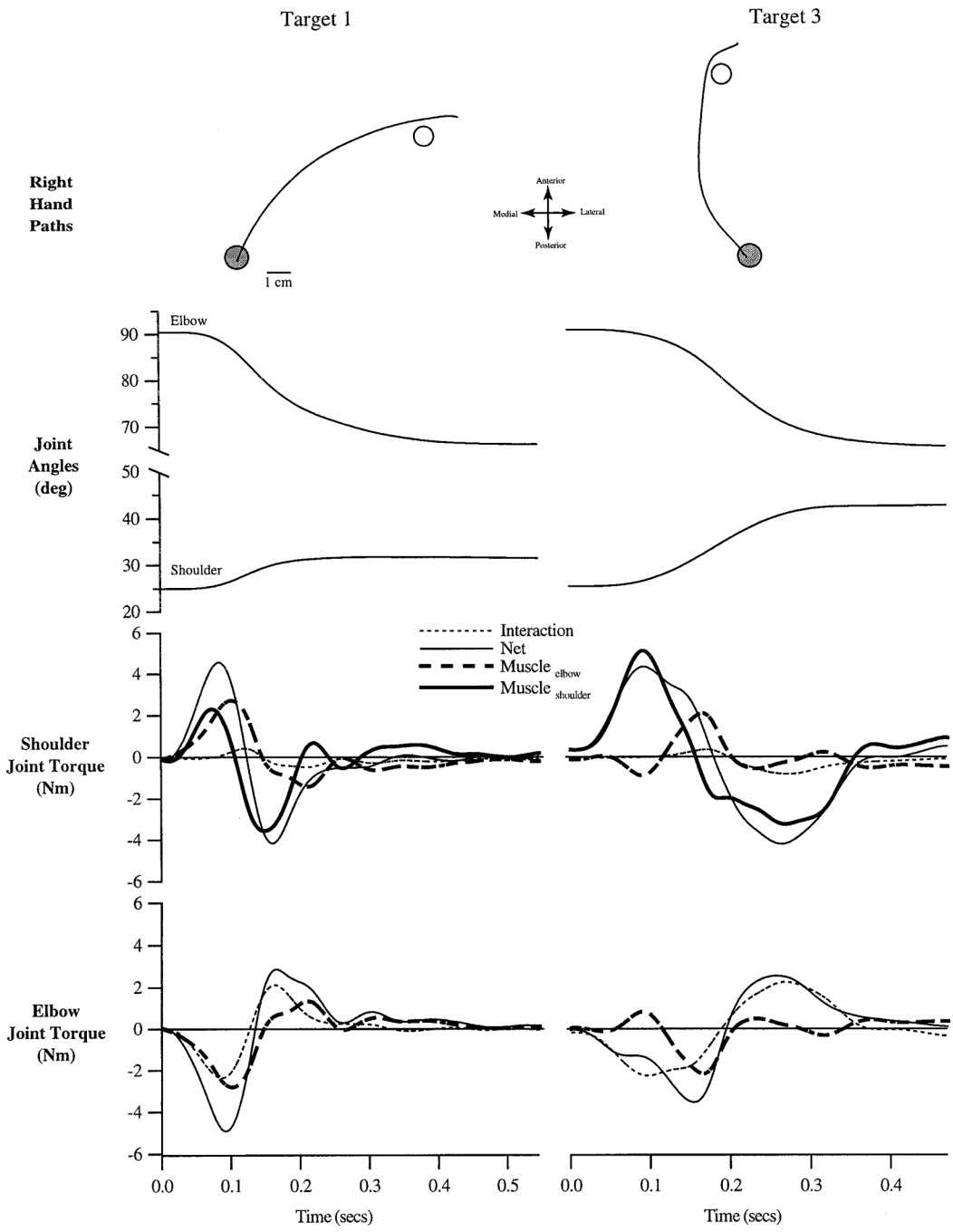

FIG. 6.

Representative trials made with the right arm to *target 1* (*left column*) and *target 3* (*right column*). Hand paths, joint angles, shoulder joint torques, and elbow joint torques (see methods) are shown. All time series data have been synchronized to movement initiation.

Author Manuscript Author Manuscript Author Manuscript Author Manuscript

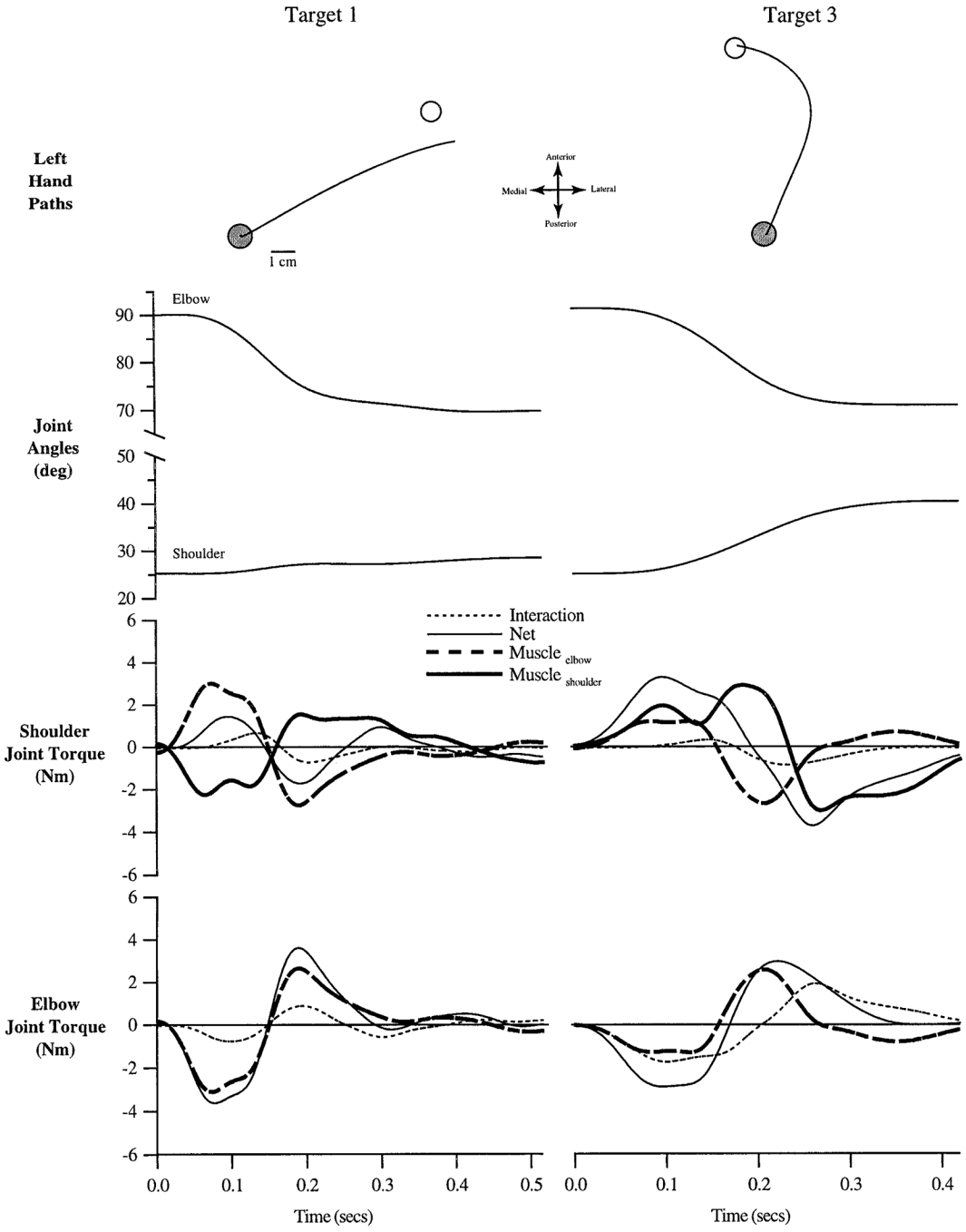

FIG. 7.

Representative trials made with the left arm to *target 1* (*left column*) and *target 3* (*right column*). Hand paths are plotted in a "right hand" coordinate system, with the medial to lateral dimension plotted along the negative to positive *x*-axis, respectively. Hand paths, joint angles, shoulder joint torques, and elbow joint torques are shown. All time series data have been synchronized to movement initiation.

Author Manuscript Author Manuscript Author Manuscript Author Manuscript

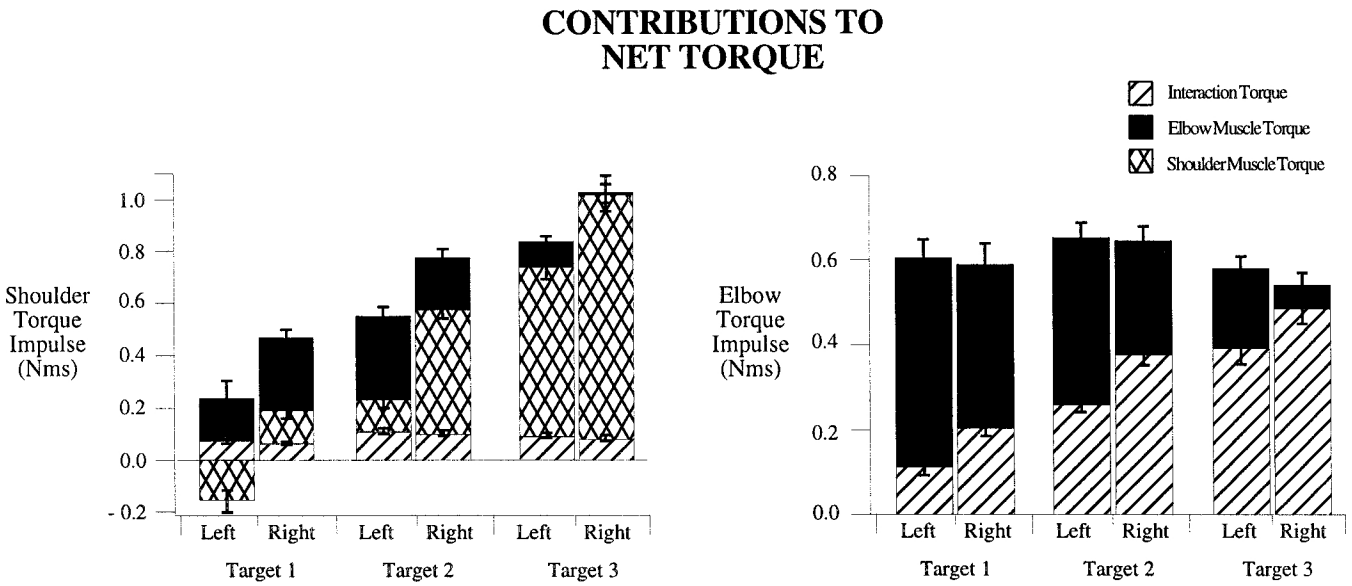

FIG. 8.

Muscle and interaction torque impulse, measured as a contribution to net torque (see methods) is shown for the shoulder (*left*) and elbow (*right*) joints. Contributions of interaction torque, elbow muscle torque, and shoulder muscle torque are plotted separately in stacked bar format. Values are averages of the individual subject means for each measure, taken separately for each limb and each target.

Author Manuscript Author Manuscript Author Manuscript Author Manuscript

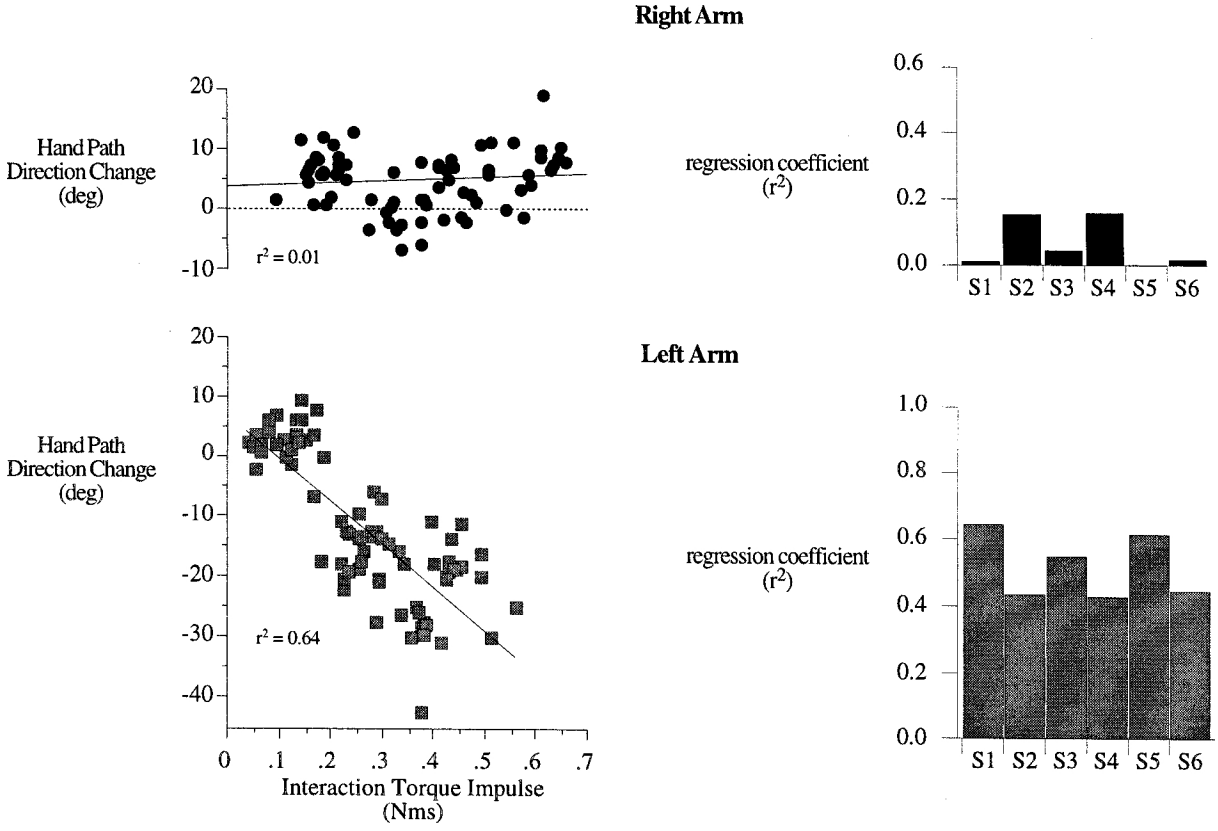

FIG. 9.

Hand path direction-change is plotted against interaction torque impulse (*left column*), taken as a contribution to net torque (see methods and Fig. 8), for all trials performed with the right arm (*top*) and left arm (*bottom*) by *subject 1*. Simple linear regressions (solid line) were performed and r^2 values are plotted in the bar plots (*right*) for trials performed with the right arm (*top*) and left arm (*bottom*) by each subject.

Author Manuscript

Author Manuscript

Author Manuscript

Author Manuscript

TABLE 1.

Percent contribution of elbow joint interaction torque impulse to elbow joint net torque impulse

	Right Arm	Left Arm
Target 1	38.8 ± 0.8	20.2 ± 0.6
Target 2	60.5 ± 0.8	42.1 ± 0.6
Target 3	93.4 ± 1.3	70.9 ± 1.0

Values are means ± SE for all subjects in percent.

Author Manuscript

Author Manuscript

Author Manuscript

Author Manuscript

Table 2.

Percent contribution of elbow joint muscle torque impulse to shoulder joint net torque impulse

	Right Arm	Left Arm
Target 1	70.2 ± 2.4	176.8 ± 5.9
Target 2	23.9 ± 1.0	58.3 ± 1.6
Target 3	2.4 ± 0.4	12.5 ± 0.8

Values are means ± SE for all subjects in percent.